



## Lithium diffusion at Si-C interfaces in silicon-graphene composites

Khorgolkhuu Odbadrakh, N. W. McNutt, D. M. Nicholson, O. Rios, and D. J. Keffer

Citation: *Applied Physics Letters* **105**, 053906 (2014); doi: 10.1063/1.4892829

View online: <http://dx.doi.org/10.1063/1.4892829>

View Table of Contents: <http://scitation.aip.org/content/aip/journal/apl/105/5?ver=pdfcov>

Published by the [AIP Publishing](#)

---

### Articles you may be interested in

Diffusion, adsorption, and desorption of molecular hydrogen on graphene and in graphite

*J. Chem. Phys.* **139**, 044706 (2013); 10.1063/1.4813919

A density functional theory study of epitaxial graphene on the (3 × 3)-reconstructed C-face of SiC

*Appl. Phys. Lett.* **102**, 093101 (2013); 10.1063/1.4794176

Atomic behavior of carbon atoms on a Si removed 3C-SiC (111) surface during the early stage of epitaxial graphene growth

*J. Appl. Phys.* **111**, 104324 (2012); 10.1063/1.4722994

Enhanced stability of hydrogen atoms at the graphene/graphane interface of nanoribbons

*Appl. Phys. Lett.* **97**, 233109 (2010); 10.1063/1.3525377

Electronic property of Na-doped epitaxial graphenes on SiC

*Appl. Phys. Lett.* **94**, 153108 (2009); 10.1063/1.3120274

---



**AIP** | Journal of  
Applied Physics

*Journal of Applied Physics* is pleased to  
announce **André Anders** as its new Editor-in-Chief

## Lithium diffusion at Si-C interfaces in silicon-graphene composites

Khorgolkhuu Odbadrakh,<sup>1</sup> N. W. McNutt,<sup>2</sup> D. M. Nicholson,<sup>3,4</sup> O. Rios,<sup>5</sup> and D. J. Keffer<sup>6</sup>

<sup>1</sup>*Joint Institute for Computational Sciences, Oak Ridge National Laboratory, Oak Ridge, Tennessee 37830, USA*

<sup>2</sup>*Department of Chemical and Biomolecular Engineering, University of Tennessee, Knoxville, Tennessee 37996, USA*

<sup>3</sup>*Computational Science and Mathematics Division, Oak Ridge National Laboratory, Oak Ridge, Tennessee 37830, USA*

<sup>4</sup>*Department of Physics, University of North Carolina, Asheville, North Carolina 28804, USA*

<sup>5</sup>*Materials Science and Technology Division, Oak Ridge National Laboratory, Oak Ridge, Tennessee 37830, USA*

<sup>6</sup>*Department of Materials Science and Engineering, University of Tennessee, Knoxville, Tennessee 37996, USA*

(Received 23 May 2014; accepted 30 July 2014; published online 8 August 2014)

Models of intercalated Li and its diffusion in Si-Graphene interfaces are investigated using density functional theory. Results suggest that the presence of interfaces alters the energetics of Li binding and diffusion significantly compared to bare Si or Graphene surfaces. Our results show that cavities along reconstructed Si surface provide diffusion paths for Li. Diffusion barriers calculated along these cavities are significantly lower than penetration barriers to bulk Si. Interaction with Si surface results in graphene defects, creating Li diffusion paths that are confined along the cavities but have still lower barrier than in bulk Si. © 2014 AIP Publishing LLC.

[<http://dx.doi.org/10.1063/1.4892829>]

The high Li absorption capacity of Si and the prominent place of Si in modern solid state technology make Si the focus of intense study for improved anode materials for Li ion batteries.<sup>1,2</sup> Very high volume expansion during lithiation, a cause for subsequent electrochemical degradation during repeated cycles, is the major limitation of Si in battery technology. It has been shown both theoretically and experimentally that this mechanical degradation can be avoided by using Si particles with sizes on the nanometer scale, mostly as a porous material formed by embedding in carbon binders.<sup>3-6</sup> However, scalability issues and a large surface area for unwanted reactions in nano engineered Si particle anode material have been identified as major stumbling blocks to mass produced battery technology.<sup>7,8</sup> On the other hand, it has been known for some time that Si micron-sized particles (hereafter referred to as microparticles) present the possibility of more affordable yet electro-mechanically sound anode materials.<sup>9,10</sup> Crystalline Si microparticles become amorphous and are pulverized into smaller sizes after the first few cycles. Surrounded by a porous carbon matrix, this combination retains both Li absorption capacity and good electrical conductivity for many cycles. A similar strategy has been reported to result in long cycle life by combining Si microparticles with a self healing polymer binder.<sup>11</sup> Recently, an electrode composed of Si microparticles in a matrix made of graphitic nanoparticles of varying sizes (carbon nano-composite) has been demonstrated to maintain very high specific capacity for more than 200 cycles.<sup>12</sup> The carbon nano-composite matrix was derived from bio-lignin presenting a further possibility of reducing the overall price of this material.

The use of Si microparticles relative to nanoparticles has an advantage over nano-engineered structures since they are easier and thus less expensive to manufacture.<sup>10</sup> Furthermore, composite materials that contain Si microparticles have the

potential for higher volumes for Li uptake compared to Si nanoparticles however the larger format Si centers are frequently reported to degrade within the first few cycles.<sup>9</sup> Anode materials based on nano- or micro-composite structures that combine high specific capacity of Si with a porous carbon matrix, have been reported to show good capacity retention and promising electrochemical performance.<sup>13</sup> The disparity in experimental based reports clearly indicates that electrochemical performance of Si-C composite anodes is critically linked to the interactions between carbon and silicon at the interfaces. A theoretical understanding of Li intercalation in these complex materials could provide significant insight and assist in the development and optimization of the next generation battery technologies. There is an extensive list of computational studies on lithiation of Si and graphite, but most of them focus on Si and graphitic carbons separately.<sup>14-20</sup> The role of Si-C interfaces in the lithiation process has been investigated very little except for cases of Si-Carbide nanotubes.<sup>21,22</sup> Si-graphene composites contain large internal surface areas in many different configurations; these internal surfaces inevitably play a role in the overall lithiation and delithiation process. In a recent report, Chou and Hwang investigated the role of single graphene sheets in Si-graphene composites and predicted that Li diffusivity near the graphene sheet to be five times larger than in bulk Li-Si alloy.<sup>23</sup> In this work, we show that Li diffusion paths could be confined by interface cavities and Graphene defects, but still offer lower diffusion barriers than that of bulk Si.

In this work, we present a Density Functional Theory (DFT) based investigation of Li diffusion at Si-graphene interfaces. Si-graphene composite has a large number of interface configurations which would require extensive combinatorial search to find the configurations that play dominant role in Li diffusion at the interface. However, we present here energetics of Li intercalation and diffusion for

carefully chosen few configurations to elucidate their role in lithiation of Si-graphene composites materials. We focus the discussion here on the more relevant chemisorption at the interfaces rather than physisorption featuring larger separation distances between Si and graphene since physisorption interfaces have little effect on Li diffusion on Si surfaces or on graphene.

The *ab-initio* calculations reported herein were performed using the DFT method within local density approximations (LDAs) as implemented in the QUANTUM-ESPRESSO code.<sup>24</sup> The pseudopotential method with a plane-wave basis set was used to describe the interaction of electrons with the ionic background. Electronic wave functions were expanded in plane waves up to an energy cutoff of 400 eV, for which energies of the configurations converged to a less than 0.1% of difference. Predicting ground states of reconstructed Si surfaces using higher order corrections such as GGA and unrestricted DFT methods have been discussed extensively in the literature.<sup>25,26</sup> These second order approximations yield ground states that differ from one another by  $\sim 0.06$  eV (Ref. 26) per dimer, which is an order of magnitude smaller than the diffusion barriers we present in this work. In addition, presence of graphene on top affects the reconstructed Si surface, rendering the much discussed buckled or symmetric ground states of pristine Si(001) surface unidentifiable. Therefore, we have limited our investigations to LDA level. Also, effects of van der Waals forces from graphene on Li diffusion near Si surface are found to have very little effect (less than 0.1% on energies) when we added them through van der Waals enabled potentials. Therefore, our report does not discuss calculations with van der Waals forces.

First, we reconstructed Si(111) ( $2 \times 2$ ) and Si(001) ( $2 \times 4$ ) surfaces using a supercell that contains six atomic layers. Dangling bonds at bottom layer terminations were passivated by hydrogen atoms fixed in space. The top layer is separated by a large distance from the periodic image of the supercell to minimize finite size effects. The surface reconstructions we obtained are in agreement with previous DFT<sup>25,27</sup> studies. The Si(001)( $2 \times 4$ ) surface relaxed into parallel chains of buckled dimers, while we added ad-atoms for Si(111) ( $2 \times 2$ ) surface reconstruction (see Fig. 1). To model the Si-graphene chemisorption interface, we relaxed a single layer of graphene parallel to Si surface and then added

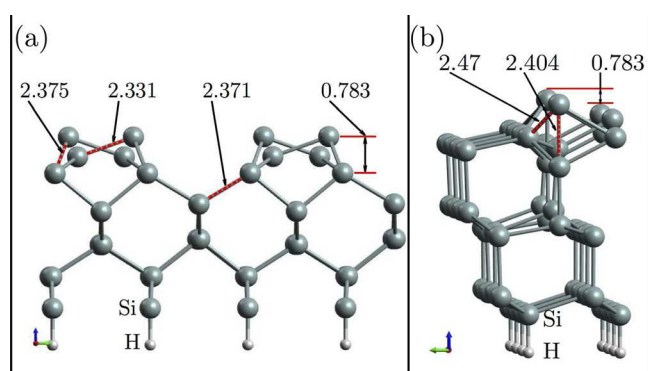


FIG. 1. Reconstructed surfaces of Si(001) (a) and Si(111) (b). Bond lengths are shown in units of Angstrom.

two more layers on top of the newly optimized structure, creating a Si-graphene interface. Size mismatch between the graphene sheet and lateral size of Si surfaces is corrected by adjusting the graphene bond lengths by not more than 3%. Optimizations with these initial conditions result in ripples or tears in the first layer of graphene after relaxation. The various relaxed configurations were used to explore the multitude of different structures present in this composite material (see Fig. 2). For example, a row of C-C bonds are broken in graphene and are bound to Si atoms from the surface dimers on Si(001) surface (see Fig. 2(b)). Other resulting configurations in the vicinity of this defect could represent interfaces formed when graphene meets a Si surface at a particular angle. The interface on Si(111) ( $2 \times 2$ ) surface shows no significant change in graphene, but does cause minor changes in bond lengths for both C and Si atoms on the surface (see Fig. 2(c)). A common feature in these interfaces is the formation of long parallel cavities etched to the Si surfaces and topped by graphene. In the case of Si(001) surface, cavities form in between dimer chains (see Figs. 2(a) and 2(b)). For Si(111) surfaces, rows of ad-atoms provide a footprint for the corridors. As mentioned before, physisorption type interfaces that feature large separation distances between Si and graphene have little effect on Li diffusion on Si surfaces or on graphene in our examinations, thus will not be discussed in this report.

After screening adsorption sites of hydrogen<sup>28,29</sup> and lithium<sup>16,30</sup> on Si surfaces as starting configurations, we identified 5 configurations for Li intercalation in Si-Gr interfaces for further optimizations. Some of the adsorption sites (ad-atom site on Si(111) surface) have been eliminated due to the addition of graphene layer on top. For Si(001) ( $2 \times 4$ )-Graphene interfaces that have no tears in the graphene layer, we identified two Li intercalation sites: one is in the cavity formed in-between two Si surface dimers (Fig. 2(1)), and the second one in-between the first two layers of graphene (Fig. 2(2)). For the Si(001) ( $2 \times 4$ )-Graphene interface that has tears in graphene, we identified two sites for Li intercalation: one is again in the Si surface cavity right at the interface (Fig. 2(3)) and the second one in the cavity formed by a graphene defect on top of the Si surface dimers (Fig. 2(4)). For Si(111) ( $2 \times 2$ )-Graphene interface, we identified only one Li intercalation site (Fig. 2(5)), which has its origin in the hydrogen adsorption site on rest-atom of Si(111) surface. Binding energies of Li at these sites (Table I) have been calculated by the formula  $E_B = E_{\text{SiGrLi}} - E_{\text{SiGr}} - E_{\text{Li}}$ , where  $E_{\text{SiGrLi}}$  is the total energy of the Si-Gr interface with Li intercalated,  $E_{\text{SiGr}}$  is the total energy of Si-Gr interface before Li is inserted, and  $E_{\text{Li}}$  is the energy of one Li atom in the same supercell as the entire system.

Nudged elastic band (NEB) method implemented in the QUANTUM-ESPRESSO code<sup>24</sup> is used to calculate diffusion barriers between equivalent Li intercalation sites. Climbing image scheme, which maximizes energy of an image along tangent of the reaction path, is used to ensure that the transition states are found correctly.

The binding energies and diffusion barriers in this report are calculated at  $T = 0^\circ\text{C}$ . The normal operating temperature of battery is near room temperature. There are numerous reports on the effects of temperature on binding energies and

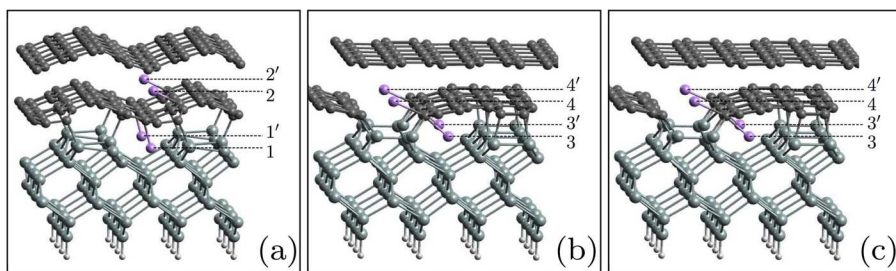


FIG. 2. Si-graphene interfaces with ripples in graphene on Si(001) surface (a), tears in graphene on Si(001) surface (b), and graphene on Si(111) surface with ad-atoms (c).

diffusion of hydrogen on Si surfaces.<sup>31,32</sup> Critical temperature of disordering for adsorbed hydrogen atom is about 1130 K on Si(111) surface,<sup>29</sup> while H hopping between adsorption sites starts at 280 °C.<sup>33</sup> So we believe, the binding energies calculated at room temperature will not differ significantly from those at room temperature.

Later in the discussion, we will report that highest diffusion barrier for Li in this system is  $\sim 0.4$  eV, which is much higher than thermal excitations at the operating temperature ( $\sim 0.025$  eV near room temperature) of batteries, therefore, only a small fraction ( $\sim \exp(0.4/0.025) = 10^{-7}$ ) of attempts would be successful in surmounting this barrier. However, the attempt frequency (roughly Debye frequency  $\sim 10^{13} \text{s}^{-1}$ ) and the density of diffusion sites on the surface result in still significant transport.

Our calculations model low coverage of Li in the system. Binding energies and diffusion barriers are somewhat reduced when the ion concentration increases.<sup>34,35</sup> However, this low coverage study has very important implications in battery manufacturing and operation, in particular for initial formation cycling, of determining the range of operating voltage for rechargeable batteries.<sup>35,36</sup>

In the next section, we will discuss energetics and diffusion characteristics of the 5 sites of Li intercalation. We would like to note again that these configurations are indeed a small representation of many possible intercalations in the Si-Graphene interface.

At the interface with the Si(001) surface, configurations 1 and 3 are known as cave sites for Li adsorption on the reconstructed Si(001) surface in the absence of graphene overlayers. These are reported to be the preferred sites for surface penetration into the bulk Si.<sup>30</sup> Binding energies of Li at sites 1 and 3 are  $-2.76$  eV and  $-2.84$  (Table I), respectively, much lower than previously reported binding energies for these sites at the bare Si(001) surface.<sup>30</sup> In the case of site (1), the topmost Si atoms that are part of the buckled

dimer chains on the Si(001) surface form a bonds to graphene, confining the Li atom intercalated in-between the dimer chains.

At the interface with Si(001), the starting position of Li atom on top of a Si rest-atom has resulted in configuration 5, with binding energy of  $-3.27$  eV (Table I), much lower than the stable binding site on bare Si(111) surface.<sup>30</sup>

Binding energies at sites 1, 3, and 5 are significantly higher in magnitude than the reported binding energies of Li in bulk Si,<sup>19</sup> which is about 1.1 eV depending on Li concentration and the nature of the amorphous Si environment. Site 5 has a binding energy 3.27 eV, higher in magnitude than even the Si-Si covalent bond energy of 2.72 eV.<sup>38</sup>

At the intercalation sites between the first and second layers of graphene, binding energies are  $-2.5$  eV and  $-3.77$  eV, respectively, for sites 2 and 4 (Table I). Site 4, situated in the valley formed by the tear in graphene, has a higher binding energy than in both bulk Si<sup>38</sup> and graphite.<sup>37,39,40</sup> Diffusion barriers between equivalent Li intercalation sites, which represent diffusion along the valleys formed at Si-graphene interfaces, are shown in Table I. Our calculations show that diffusion barriers along these paths are comparable to barriers on Si surfaces with similar binding sites: 0.21 eV for Si(001) and 0.5 eV for Si(111) surfaces. The presence of graphene also alters diffusion paths slightly, resulting in non-symmetric reaction transition curves (see Fig. 3). However, the calculated diffusion barriers are significantly lower than the barriers to diffusion into both bulk silicon and graphite.

A small number of representative configurations representing Si-Graphene interfaces have been investigated for

TABLE I. Absorption energy and diffusion barrier for Li intercalation sites in Si-Graphene interface. See Fig. 2 for site labels.

Site	Energy (eV)	Barrier (eV)	Site'
1	-2.76	0.41	1'
2	-2.50	0.10	2'
3	-2.84	0.21	3'
4	-3.77	0.15	4'
5	-3.27	0.41	5'
Bulk Si <sup>19</sup>	$\sim -1.1$	$\sim 0.58$	
Graphite <sup>37</sup>	$\sim -2.75$	$\sim 0.5$	
Si(001) penetration <sup>19</sup>		$\sim 1.13$	
Si(111) penetration <sup>19</sup>		$\sim 0.56-1.26$	

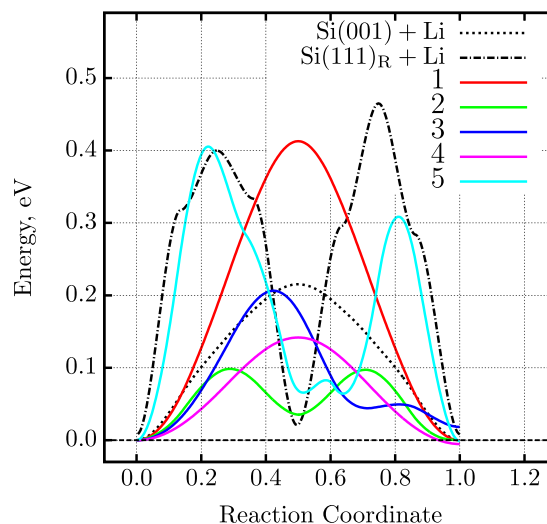


FIG. 3. Diffusion barriers at Si-Graphene interface. The two dashed lines are for Li diffusion on Si surfaces.

intercalation of Li. Results suggest that the presence of chemisorption type interfaces between Si and Graphite alter energetics of Li binding significantly compared to bare Si or Graphene surfaces. Some of the sites are energetically more favorable than sites in bulk Si or graphite. On the other hand, diffusion barriers calculated along the interface cavities are lower than the bare Si or graphene surfaces. However, the calculated diffusion barriers and penetration barriers into the bulk Si may be lower in high concentration lithiation processes as pointed out by Kaghazchi.<sup>41</sup> Higher binding energy combined with lower diffusion barriers suggest that binary interfaces formed in the Si-graphene composite materials may be playing a role in lithiation/delithiation or relithiation processes, and 3D structures at nanometer scales such as carbon nanotubes may not be the only structure for high performing Li-ion battery technology. Our results broadly agree with findings of Chou and Hwang,<sup>23</sup> which predicted that Li diffusivity near the graphene sheet to be two dimensional and five times larger than in bulk Li-Si alloy. In addition, our results show that interface cavities and Graphene defects provide additional confinements to Li diffusion paths, but still offer lower diffusion barriers than in the bulk Si. The rate performance and intercalation related stresses are directly related to the diffusion and distribution of Li-ions within the active material and interfaces. A typical engineering solution is to circumvent the issues associated with poor transport dynamics by incorporating nano-materials in lieu of micron scale particles thereby minimize the solid state diffusion length. We have shown that defect sites within Si/graphene interfaces result in energetics that are more favorable for high performance Li-ion battery technology. Therefore, we expect that the manufacturing of Si-carbon composites with abundant “special” interfaces will enhance the electrochemical performance and cyclic stability of the high capacity Si-C anode. This study reveals an alternative to nano-silicon architectures and indicates that microstructural optimization of nano-crystalline carbon on pristine crystalline Si will maximize the occurrence of these special sites and is a prospective route to bulk composite anodes with nano-material enabled performance.

K.O. was supported by a grant from the JDRD program at the University of Tennessee. N.M. was supported by a grant from the Oak Ridge Associated Universities High Performance Computing Program, by a grant from the Sustainable Energy Education and Research Center of the University of Tennessee and by a grant from the National Science Foundation (DGE-0801470). This research project used resources of the National Institute for Computational Sciences (NICS) supported by NSF under Agreement No. OCI 07-11134.5. This research was also sponsored in part by the Laboratory Directed Research and Development Program of Oak Ridge National Laboratory, managed by UT-Battelle, LLC, for the U. S. Department of Energy.

- <sup>1</sup>C. Wen and R. A. Huggins, *J. Solid State Chem.* **37**, 271 (1981).
- <sup>2</sup>M. Obrovac and L. Christensen, *Electrochem. Solid State Lett.* **7**, A93 (2004).
- <sup>3</sup>C. K. Chan, H. Peng, G. Liu, K. McIlwrath, X. F. Zhang, R. A. Huggins, and Y. Cui, *Nat. Nanotechnol.* **3**, 31 (2008).
- <sup>4</sup>A. Magasinski, P. Dixon, B. Hertzberg, A. Kvit, J. Ayala, and G. Yushin, *Nat. Mater.* **9**, 353 (2010).
- <sup>5</sup>Y. Yao, M. T. McDowell, I. Ryu, H. Wu, N. A. Liu, L. B. Hu, W. D. Nix, and Y. Cui, *Nano Lett.* **11**, 2949 (2011).
- <sup>6</sup>W. Wang and P. N. Kumta, *J. Power Sources* **172**, 650 (2007).
- <sup>7</sup>J. B. Goodenough and Y. Kim, *Chem. Mater.* **22**, 587 (2010).
- <sup>8</sup>A. Arico, P. Bruce, B. Scrosati, J. Tarascon, and W. Van Schalkwijk, *Nat. Mater.* **4**, 366 (2005).
- <sup>9</sup>J. Saint, M. Morcrette, D. Larcher, L. Laffont, S. Beattie, J.-P. Peres, D. Talaga, M. Couzi, and J.-M. Tarascon, *Adv. Funct. Mater.* **17**, 1765 (2007).
- <sup>10</sup>M. N. Obrovac and L. J. Krause, *J. Electrochem. Soc.* **154**, A103 (2007).
- <sup>11</sup>C. Wang, H. Wu, Z. Chen, M. T. McDowell, Y. Cui, and Z. A. Bao, *Nat. Chem.* **5**, 1043 (2013).
- <sup>12</sup>O. Rios, S. K. Martha, M. A. McGuire, W. Tenhaeff, K. More, C. Daniela, and J. Nandaa, “Direct Synthesis and fabrication of C-Si-SiO<sub>2</sub> Monolithic Composite Electrodes Comprised of Lignin-derived Carbon Fibers Embedded with Silicon,” *Energy Technol. J.* (to be published).
- <sup>13</sup>B. Scrosati, J. Hassoun, and Y.-K. Sun, *Energy Environ. Sci.* **4**, 3287 (2011).
- <sup>14</sup>S. C. Jung, J. W. Choi, and Y.-K. Han, *Nano Lett.* **12**, 5342 (2012).
- <sup>15</sup>O. I. Malyi, T. L. Tan, and S. Manzhos, *Appl. Phys. Express* **6**, 027301 (2013).
- <sup>16</sup>M. K. Y. Chan, C. Wolverton, and J. P. Greeley, *J. Am. Chem. Soc.* **134**, 14362 (2012).
- <sup>17</sup>Q. Zhang, Y. Cui, and E. Wang, *J. Phys. Chem. C* **115**, 9376 (2011).
- <sup>18</sup>P. Johari, Y. Qi, and V. B. Shenoy, *Nano Lett.* **11**, 5494 (2011).
- <sup>19</sup>K. Zhao, W. L. Wang, J. Gregoire, M. Pharr, Z. Suo, J. J. Vlassak, and E. Kaxiras, *Nano Lett.* **11**, 2962 (2011).
- <sup>20</sup>M. Khantha, N. Cordero, L. Molina, J. Alonso, and L. Girifalco, *Phys. Rev. B* **70**, 125422 (2004).
- <sup>21</sup>X. Wang and K. M. Liew, *J. Phys. Chem. C* **116**, 26888 (2012).
- <sup>22</sup>Q. Si, K. Hanai, N. Imanishi, M. Kubo, A. Hirano, Y. Takeda, and O. Yamamoto, *J. Power Sources* **189**, 761 (2009).
- <sup>23</sup>C.-Y. Chou and G. S. Hwang, *J. Phys. Chem. C* **117**, 9598 (2013).
- <sup>24</sup>P. Giannozzi, S. Baroni, N. Bonini, M. Calandra, R. Car, C. Cavazzoni, D. Ceresoli, G. L. Chiarotti, M. Cococcioni, I. Dabo *et al.*, *J. Phys.: Condens. Matter* **21**, 395502 (2009).
- <sup>25</sup>S. Solares, S. Dasgupta, P. Schultz, Y. Kim, C. Musgrave, and W. Goddard, *Langmuir* **21**, 12404 (2005).
- <sup>26</sup>S. Back, J. A. Schmidt, H. Ji, J. Heo, Y. Shao, and Y. Jung, *J. Chem. Phys.* **138**, 204709 (2013).
- <sup>27</sup>X. Luo, G. Qian, C. Sagui, and C. Roland, *J. Phys. Chem. C* **112**, 2640 (2008).
- <sup>28</sup>M. Duerr and U. Hofer, *Prog. Surf. Sci.* **88**, 61 (2013).
- <sup>29</sup>A. Vittadini and A. Selloni, *Phys. Rev. Lett.* **75**, 4756 (1995).
- <sup>30</sup>S. C. Jung and Y.-K. Han, *Phys. Chem. Chem. Phys.* **13**, 21282 (2011).
- <sup>31</sup>J. Xie, N. Imanishi, T. Zhang, A. Hirano, Y. Takeda, and O. Yamamoto, *Mater. Chem. Phys.* **120**, 421 (2010).
- <sup>32</sup>G. A. Tritsarlis, E. Kaxiras, S. Meng, and E. Wang, *Nano Lett.* **13**, 2258 (2013).
- <sup>33</sup>R. L. Lo, M. S. Ho, I. S. Hwang, and T. T. Tsong, *Phys. Rev. B* **58**, 9867 (1998).
- <sup>34</sup>A. J. Morris, C. P. Grey, R. J. Needs, and C. J. Pickard, *Phys. Rev. B* **84**, 224106 (2011).
- <sup>35</sup>W.-J. Zhang, *J. Power Sources* **196**, 13 (2011).
- <sup>36</sup>M. Park, X. Zhang, M. Chung, G. B. Less, and A. M. Sastry, *J. Power Sources* **195**, 7904 (2010).
- <sup>37</sup>A. Marquez, A. Vargas, and P. Balbuena, *J. Electrochem. Soc.* **145**, 3328 (1998).
- <sup>38</sup>B. Farid and R. Godby, *Phys. Rev. B* **43**, 14248 (1991).
- <sup>39</sup>D. P. Divincenzo and E. J. Mele, *Phys. Rev. Lett.* **53**, 52 (1984).
- <sup>40</sup>F. Valencia, A. H. Romero, F. Ancilotto, and P. L. Silvestrelli, *J. Phys. Chem. B* **110**, 14832 (2006).
- <sup>41</sup>P. Kaghazchi, *Appl. Phys. Lett.* **102**, 093901 (2013).